ACS Medicinal Chemistry Letters

pubs.acs.org/acsmedchemlett

Discovery of an Orally Efficacious Imidazo[5,1-*f*]-[1,2,4]triazine Dual Inhibitor of IGF-1R and IR

Meizhong Jin,*[,†] Prafulla C. Gokhale,[‡] Andy Cooke,[‡] Kenneth Foreman,[†] Elizabeth Buck,[†] Earl W. May,[†] Lixin Feng,[‡] Mark A. Bittner,[‡] Mridula Kadalbajoo,[†] Darla Landfair,[‡] Kam W. Siu,[†] Kathryn M. Stolz,[†] Douglas S. Werner,[†] Radoslaw S. Laufer,[†] An-Hu Li,[†] Hanqing Dong,[†] Arno G. Steinig,[†] Andrew Kleinberg,[†] Yan Yao,[†] Jonathan A. Pachter,[†] Robert Wild,[‡] and Mark J. Mulvihill*[,†]

[†]OSI Oncology, OSI Pharmaceuticals, Inc., 1 Bioscience Park Drive, Farmingdale, New York 11735, and
[‡]OSI Oncology, OSI Pharmaceuticals, Inc., 2860 Wilderness Place, Boulder, Colorado 80301

ABSTRACT This report describes the investigation of a series of 5,7-disubstituted imidazo[5,1-*f*][1,2,4]triazine inhibitors of insulin-like growth factor-1 receptor (IGF-1R) and insulin receptor (IR). Structure−activity relationship exploration and optimization leading to the identification, characterization, and pharmacological activity of compound **9b**, a potent, selective, well-tolerated, and orally bioavailable dual inhibitor of IGF-1R and IR with in vivo efficacy in tumor xenograft models, is discussed.

KEYWORDS Insulin-like growth factor-1 receptor (IGF-1R), insulin receptor (IR), inhibitors, structure-based drug design (SBDD), cancer

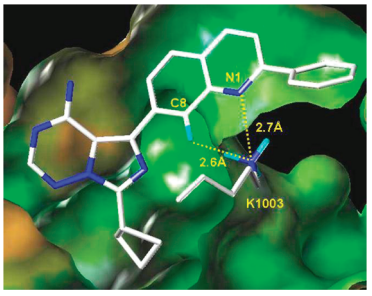

Insulin-like growth factor-1 receptor (IGF-1R) is a tetrameric transmembrane receptor tyrosine kinase activated by the binding of its cognate ligands IGF-1 and IGF-2.[1,2] Preclinical studies show that activation of IGF-1R is required for cellular transformation and tumorigenesis, and inhibition of IGF-1R activity results in reduced growth of tumor xenografts.[3−8] The importance of IGF-1R as an anticancer target is further underscored by its role in promoting resistance to cytotoxic chemotherapies, as well as molecular targeted therapies including HER2 and EGFR antagonists.[3,9−13] Validation of IGF-1R as an anticancer target has been demonstrated by several monoclonal antibodies directed against the receptor's extracellular ligand binding domain in the clinical setting.[14] However, efficacy mediated by IGF-1R-selective MAbs may be limited due to lack of coverage on the structurally related insulin receptor (IR). A growing body of data supports the importance of the IR in tumor cell proliferation and survival. Increased expression of IR is observed in several types of human cancers, and activation of IR by either insulin or IGF-2 results in enhanced proliferation of select human tumor cell lines.[7,15−19] Moreover, bidirectional cross-talk between IGF-1R and IR can occur whereby inhibition of either receptor individually results in a compensatory increase in the phosphorylation state of the reciprocal receptor. For xenografts coexpressing IGF-1R and IR, dual inhibition of both receptors results in greater antitumor activity as compared to inhibiting IGF-1R alone.[20] These results have provided a rationale for dual IGF-1R/IR inhibition as a treatment of cancer.

Recently, small molecular kinase inhibitors targeting both IGF-1R and IR have been developed and advanced into clinical studies.[21] We have previously disclosed our work around imidazo[1,5-*a*]pyrazine derived small molecule dual IGF-1R/IR inhibitors, including the discovery of OSI-906, which is currently in advanced clinical development (Figure 1).[22,23] While the main thrust of our IGF-1R/IR small molecule drug discovery efforts focused primarily on the imidazopyrazine series, alternate bioisosteric cores were also considered. Herein, we report the discovery of imidazo[5,1-*f*][1,2,4]triazine-based inhibitors of IGF-1R and IR and, particularly, compound **9b** as a potent, selective, orally bioavailable dual IGF-1R and IR inhibitor with in vivo efficacy in mouse xenograft models.

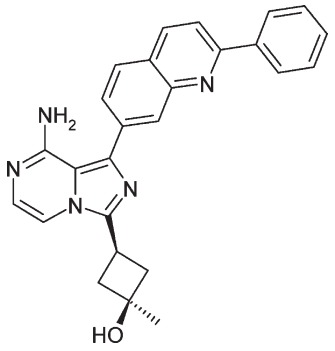

Figure 1. OSI-906.

As shown in Scheme 1, the initial proof-of-concept 5,7-disubstituted imidazo[5,1-*f*][1,2,4]triazine compound **1a** was synthesized via a Suzuki coupling of intermediate **2** (X = N)[24] with boronate **3a**. Compound **1a** showed activity against IGF-1R both biochemically and cellularly (Table 1). However, a

Received Date: July 23, 2010
Accepted Date: August 14, 2010
Published on Web Date: August 30, 2010

DOI: 10.1021/ml100178g | *ACS Med. Chem. Lett.* **2010**, *1*, 510–515

ACS Medicinal Chemistry Letters
pubs.acs.org/acsmedchemlett

Scheme 1. Synthesis of Imidazo[5,1-*f*][1,2,4]triazine IGF-1R Inhibitor **1a**[a]

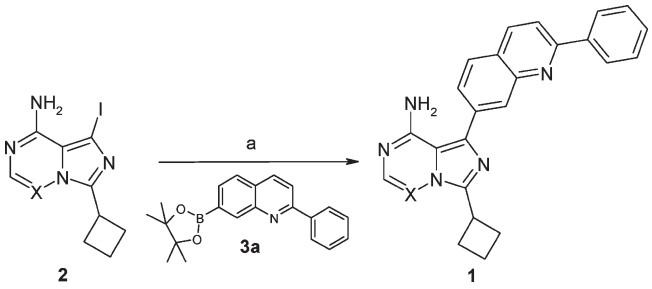

[a]Reagents and conditions: (a) $PdCl_2$(dppf), K_2CO_3, dioxane−water (4:1, v:v), 95 °C, 70−75%.

Table 1. In Vitro Potency and Microsomal Stability of Compounds **1a** and **1b**

compound	X	IGF-1R biochemical[a] IC_{50} (μM)	IGF-1R cell mechanistic[b] IC_{50} (μM)	extraction ratios	
				mouse	human
1a	N	0.27	0.33	0.89	0.91
1b	CH	0.079	0.086	0.88	0.85

[a]A 100 μM concentration of ATP. [b] LISN cell line.

significant loss in potency was observed as compared to its counterpart **1b**, an early lead compound from the imidazo[1,5-*a*]pyrazine series from which OSI-906 emerged.[22] We hypothesized that the decrease in potency derived from weaker hinge hydrogen-bonding interactions due to a reduction in the electron richness of the donor and acceptor in **1a** as compared to **1b**. Differences in desolvation between the two agents may also play a contributing role. In either event, our efforts focused on increasing the potency through further modifications to **1a**.

To expedite the lead optimization process, we decided to generate a focused library based on the structural insights and structure−activity relationship (SAR) developed around the earlier imidazo[1,5-*a*]pyrazine series.[22,23] In that series, a hydrogen bond between the quinoline nitrogen and the basic amine of Lys1003, in addition to the hydrogen bonds to the hinge, are critical for activity. Furthermore, the imidazopyrazine C3 substituent, which exited out to solvent, allowed for the control of overall drug metabolism and pharmacokinetic (DMPK) properties. Hence, in the imidazotriazine series, improving the quinoline's acceptor pharmacophore became the major focus for improving potency. The C7 substituent was limited to three preferred substituted cyclobutyl analogues, which showed favorable DMPK properties and maintained both IGF-1R and IR target potency within the imidazopyrazine series. Detailed consideration of the quinoline's interaction with Lys1003 led to the hypothesis that a hydrogen bond acceptor at the C8 position of the quinolinyl moiety could further strengthen this interaction and thus enhance activity (Figure 2). The space adjacent to the C8 position is sterically congested, limiting replacements of the C8-H to either N8 or C8-F. Fluorine substitution is

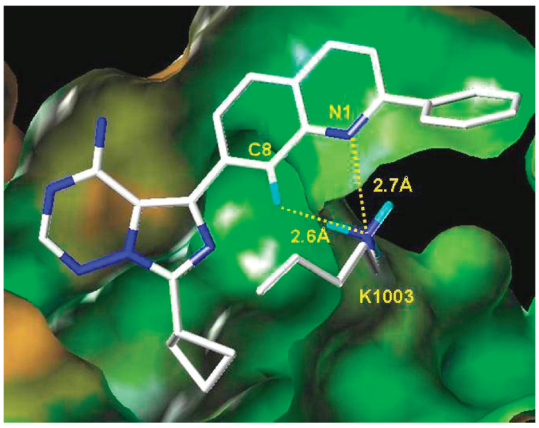

Figure 2. Modeled interaction of the quinoline moiety of **1a** with the catalytic lysine (K1003) of IGF-1R.[25] The lysine nitrogen is closer to the C8-H than to the N1. One proton points directly to the C8-H position in the lowest energy rotamer of the amine (depicted), while a nearly eclipsed conformation is required to point a proton directly at the N1 position.

preferred, as the fluorine serves as a hydrogen bond acceptor, has small van der Waals volume, is metabolically inert, and approaches closer to the basic amine on K1003 than the lone pair on a ring nitrogen would.

The synthetic chemistry used to prepare these advanced imidazotriazine analogues is shown in Scheme 2. Amide **6** was prepared from coupling of 5-methoxy-[1,2,4]triazin-6-ylmethylamine **4**[24] with the activated cyclobutanone ester **5**. Subsequent $POCl_3$ cyclization followed by bromination afforded common intermediate **7**. The cyclobutanone moiety of **7** was converted to a tertiary alcohol via a Grignard reaction yielding the cis-isomer stereoselectively. Ammonolysis gave compound **8**, and compound **9** was obtained after a Suzuki coupling of **8** with boronate **3**. Alternatively, **7** was subjected to ammonolysis followed by reductive amination to provided compound **10**, which went on to a Suzuki coupling with boronate **3** to give final compound **11**.

As shown in Table 2, the addition of a fluorine atom at the C8 position of the quinoline ring boosted potency, in accord with the binding affinity hypothesis. These compounds inhibited IR and IGF-1R with similar potencies and showed improved in vitro microsomal stability when compared to **1a**.

On the basis of their in vitro profiles, compounds **9b**, **11b**, and **11d** were prioritized for mouse PK evaluation at 5 mg/kg for iv dose and 25 mg/kg for oral dose. Key mouse PK parameters for these compounds are summarized in Table 3. Compounds **11b** and **11d** showed lower exposure and bioavailability as compared to **9b**, presumably due to their lower permeability as indicated by PAMPA data, especially at lower pH. The apparent oral bioavailability in excess of 100% for **9b** may indicate saturation of a clearance mechanism. On the basis of its overall in vitro and DMPK profile, **9b** was selected for further profiling.

The in vitro and in vivo drug discovery cascade focused primarily on a GEO human colorectal tumor cell line. The GEO cell line was chosen since it represents a naturally occurring IGF-1R/IR/IGF2 autocrine loop driven tumor line

DOI: 10.1021/ml100178g | *ACS Med. Chem. Lett.* **2010**, *1*, 510–515

Scheme 2. General Synthesis Scheme[a]

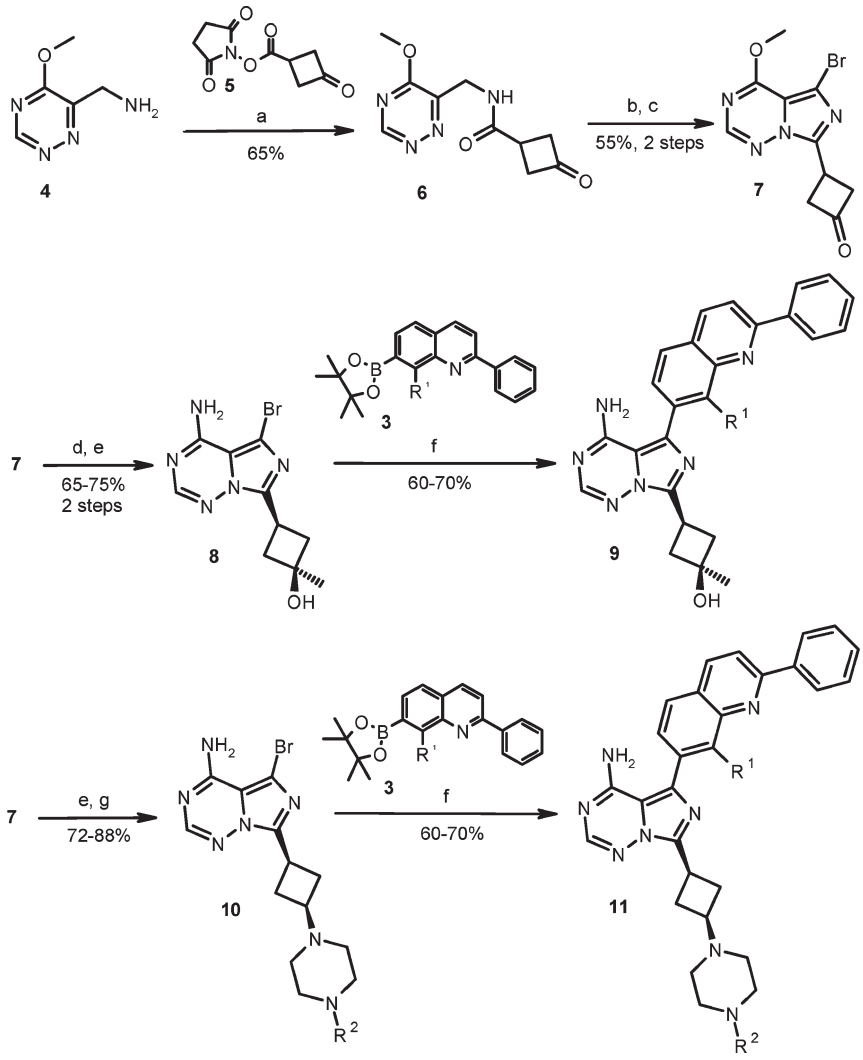

[a]Reagents and conditions: (a) 10% aqueous $NaHCO_3$, THF, room temperature. (b) $POCl_3$, DMF/MeCN, room temperature. (c) NBS, DMF. (d) MeMgCl, THF, −78 °C. (e) 2 N NH_3 in iPrOH, 50 °C. (f) $PdCl_2$(dppf), K_2CO_3, dioxane−water (4:1, v:v), 95 °C. (g) 1-Methylpiperazine or 1-formylpiperazine, $NaBH(OAc)_3$, THF, room temperature.

Table 2. Further SAR Explorations

	R^1	R^2	IGF-1R cell mechanistic[a] IC_{50} (μM)	IR cell mechanistic[b] IC_{50} (μM)	extraction ratios mouse	extraction ratios human
9a	H		0.15	0.70	0.62	0.71
9b	F		0.017	0.076	0.43	0.55
11a	H	CHO	0.026	0.26	0.24	0.66
11b	F	CHO	0.008	0.048	0.44	0.65
11c	H	CH_3	0.025	0.32	0.52	0.64
11d	F	CH_3	0.014	0.068	0.44	0.50

[a]LISN cell line. [b] HepG2 cell line.

Table 3. PAMPA Permeability and Mouse PK[a] of **9b**, **11b**, and **11d**

	PAMPA (nm/s)		5 mg/kg iv dose		25 mg/kg po dose	
	pH 5.0	pH 7.4	Cl (mL/min/kg)	V_{ss} (L/kg)	C_{max}(μM)	*F* %
9b	1090	1100	4	1.0	20.5	162
11b	204	1050	7	1.2	3.1	18
11d	145	672	21	4.9	1.9	27

[a]Compounds were dosed as freebase in female CD-1 mice.

and is sensitive to dual inhibition of IGF-1R and IR.[26] Moreover, the line forms tumors in vivo and is an ideal model for tumor growth inhibition studies where the degree and duration of in vivo inhibition of tumor IGF-1R/IR phosphorylation could be correlated to in vivo efficacy. In this GEO cell line, **9b** fully inhibited phosphorylation of IGF-1R and IR in vitro in a dose-dependent manner (Figure 3a), leading to downstream inhibition of pAKT (Figure 3b), with antiproliferative effects correlating with IR and IGF-1R inhibition (EC_{50} = 130 nM).

DOI: 10.1021/ml100178g | *ACS Med. Chem. Lett.* **2010**, *1*, 510–515

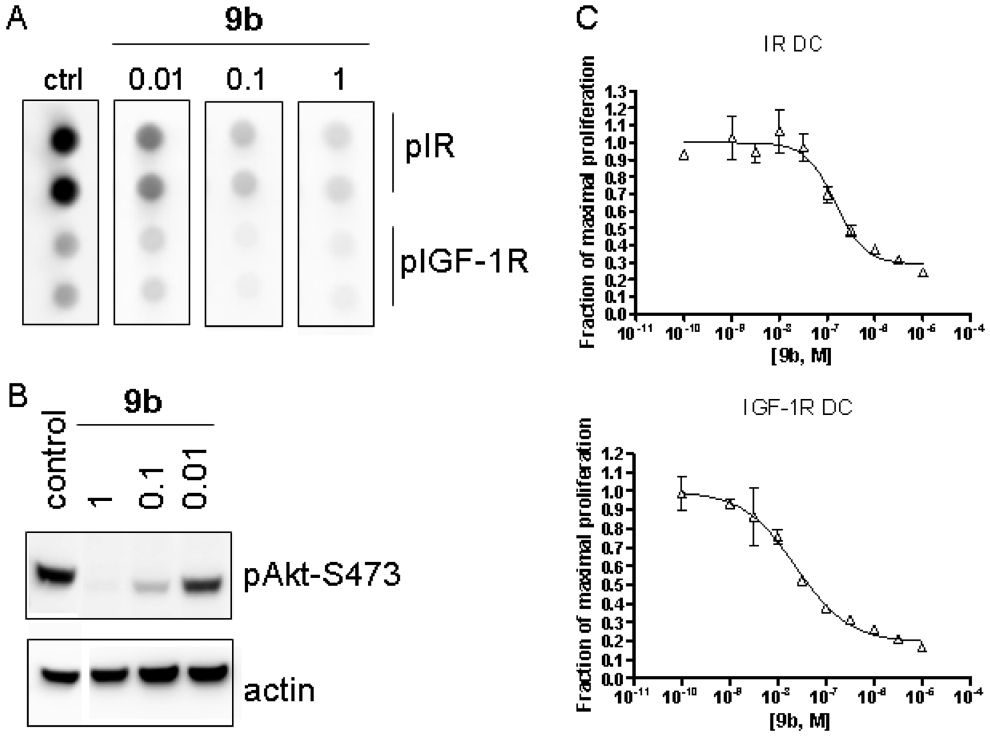

Figure 3. Inhibition of cellular signaling and proliferation by **9b**. (a) Effect of varying concentrations of **9b** on IGF-1R and IR phosphorylation in human GEO tumor cells. (b) Effect of varying concentrations of **9b** on pAkt in human GEO tumor cells. (c) Effect of varying concentrations of **9b** on cell proliferation for IR and IGF-1R DC tumor cell models.

Table 4. Median Pharmacokinetic Parameters for Compound **9b** Following Oral Administration in Different Species

species	dose (mg/kg)	C_{max} (μM)	AUC (ng h/mL)	CL (mL/min/kg)[c]	V_{ss} (L/kg)[c]	F %
rat (F)	25[a]	11.3	62415	4	0.97	64
rhesus monkey (M)	30[b]	10.8	31383	15	0.55	97
mouse (F)	25[b]	35.2	240013	4	1.00	100

[a] Free base of **9b** was dosed; vehicle, 50:50 PEG-400:25 mM tartaric acid. [b] HCl salt of **9b** was dosed; vehicle, 40 % w/v hydroxypropyl-β-cyclodextrin (Trappsol). [c] A 5 mg/kg iv dose.

Furthermore, compound **9b** was profiled in IGF-1R and IR driven DC tumor cell lines[27] in vitro and emulated the observations observed in the GEO line, with antiproliferative effects in both lines correlating with inhibition of both pIGF-1R and pIR (Figure 3c). When taken together, these results indicate that inhibition of IGF-1R and IR leads to inhibition of downstream signaling of Akt, which results in the inhibition of proliferation in IGF-1R and IR driven cell lines in vitro.

The pharmacokinetics of **9b** was evaluated in multiple species, including rat and rhesus monkey. As shown in Table 4, **9b** demonstrated low clearance, good bioavailability, and good exposure in these two species when dosed orally once a day. In dose escalating PK studies, **9b** gave dose proportional exposure in these species (data not shown). Repeated oral dosing in mouse, rat, and monkey did not show any evidence of a systematic increase or decrease in exposure as compared to single doses. Additionally, optimization of the salt form and dose vehicle was carried out on **9b**. The combination of the hydrochloride salt of **9b** and 40 % w/v of hydroxypropyl-β-cyclodextrin (Trappsol) as the vehicle resulted in a solubility of approximately 60 mg/mL. A slight increase in exposure was observed in mice when compared to the free base form (Table 4). Thus, the HCl salt of **9b** in combination with the 40 % w/v of hydroxypropyl-β-cyclodextrin (Trappsol) as the vehicle was used in further in vivo profiling studies.

Pharmacokinetic/pharmacodynamic evaluation of **9b** in vivo in the GEO colon carcinoma xenograft model demonstrated that a single oral dose of 10 mg/kg provided > 70 % sustained inhibition of tumor IGF-1R phosphorylation up to 8 h, corresponding to plasma levels of > 4 μM. Partial recovery of pIGF-1R content (50 % inhibition at 16 h) was observed with a concomitant drop in the plasma drug levels to 0.38 μM by 16 h (Figure 4a). Similar inhibitory effects of **9b** on tumor insulin receptor phosphorylation were observed (Figure 4a). Twice daily administration at a dose of 10 mg/kg for 14 days resulted in 91 % tumor growth inhibition (TGI) in the GEO model (Figure 4b). Furthermore, a once daily dose of 20 mg/kg resulted in comparable TGI of 85 % (Figure 4b), whereas 5 mg/kg bid only provided 31 % TGI. The compound was well tolerated with limited body weight loss (< 10 %). In this TGI study, tumors from control and **9b** treated animals were removed after the last dose to investigate target

DOI: 10.1021/ml100178g | ACS Med. Chem. Lett. 2010, 1, 510–515

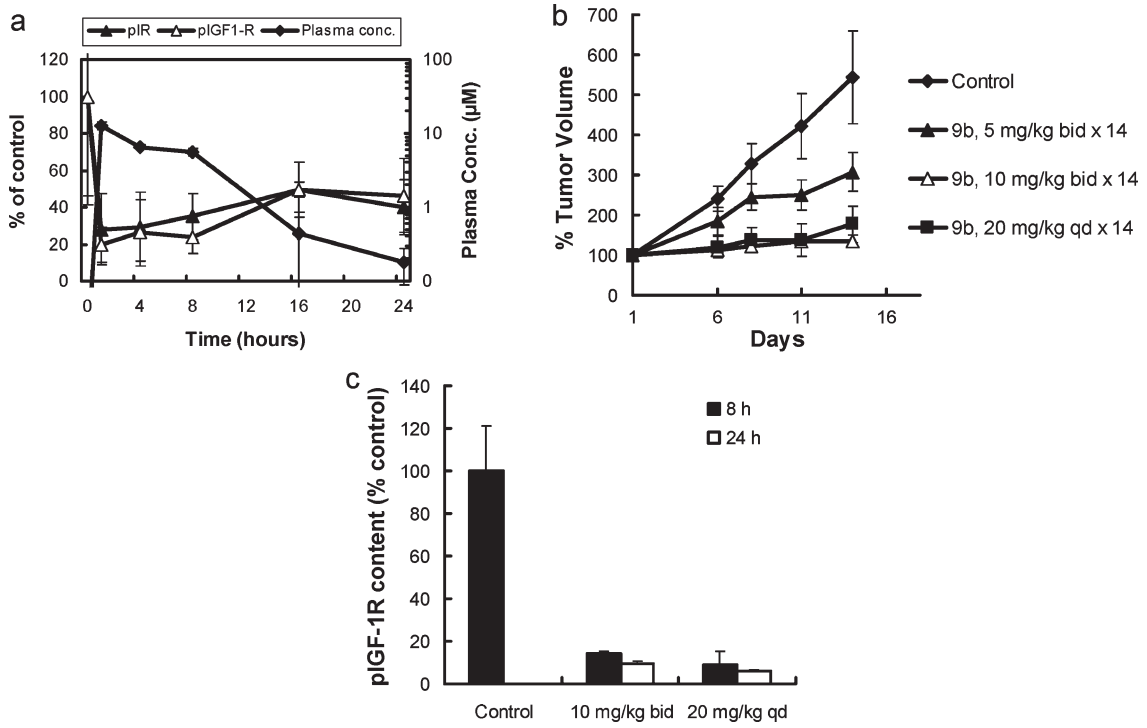

Figure 4. (a) Correlation of inhibition of IGF-1R and IR phosphorylation and plasma drug concentration in GEO tumor xenografts following oral dosing with 10 mg/kg of **9b**. The plotted data are means ± SDs. Phospho-IGF-1R and pIR contents in GEO tumors are expressed as a percentage of control pIGF-1R or pIR content from vehicle-treated animals, respectively. (b) Dose−response efficacy of **9b** in GEO xenograft models. Plotted data are mean tumor volumes expressed as a percentage of initial volume ± SE. Compound **9b** was dosed on a once daily (qd) or twice daily (bid) schedule for 14 days. (c) Inhibition of IGF-1R phosphorylation in GEO tumor xenografts following 14 days of oral dosing with **9b**. Data are means ± SEs.

inhibition in tumor tissue. Compound **9b** at the efficacious doses of 10 mg/kg bid or 20 mg/kg qd provided > 70−90% sustained inhibition of tumor IGF-1R phosphorylation for a full 24 h post last dose (Figure 4c). At the lower, nonefficacious dose of 5 mg/kg bid for 14 days, only 40−50% pIGF-1R and pIR inhibition was observed (data not shown), suggesting that near complete and sustained target inhibition may be required for maximum efficacy in this IGF-1R/IR driven model. Blood glucose and insulin levels were also measured after the last dose showing only transient elevation up to 8 h with return to normal levels by 24 h for the efficacious dose levels. The antitumor activity of **9b** was extended into additional tumor models. For example, in a human IGF-1R overexpressing NIH 3T3 xenograft model (LISN), **9b** demonstrated 100% TGI when dosed at a well-tolerated dose of 10 mg/kg bid for 14 days (data not shown).

The kinase selectivity of **9b** was determined by screening against a panel 167 kinases using an in-house Caliper EZ Reader mobility shift assay. Compound **9b** only showed significant activity (> 50% inhibition at 1 μM concentration) against IGF-1R and IR.[28] Compound **9b** did not show any significant CYP inhibition against major CYP isoforms (Table 5). Preclinical safety screens of **9b** against a broad range of 68 enzymes, receptors, and ion channels at 10 μM concentration did not reveal any significant off-target activities. Thus, **9b** is a highly selective dual IGF-1R/IR inhibitor. The plasma protein binding as measured by ultracentrifugation for **9b** in multiple species was moderate (Table 5). Compound **9b** is not genotoxic

Table 5. Plasma Protein Binding and Cytochrome P450 Inhibition of **9b**

plasma protein binding (ultracentrifugation)	%	CYP isoform	IC_{50} (μM)
mouse	98.5	3A4	> 25.0
rat	96.6	1A2	> 25.0
human	97.3	2D6	> 25.0

(Ames negative ± S9) and showed no detectable off-target toxicological effects in a 14 day rat toxicology study, even at doses and exposures above those predicted to be required for efficacy.

In summary, a 5,7-disubstituted imidazo[5,1-*f*][1,2,4]triazine series was conceived as an isosteric alternative to the imidazo[1,5-*a*]pyrazine dual IGF-1R/IR inhibitors. Optimization of the interactions with K1003 compensated for the observed potency loss due to the core change. Further chemical modifications improved the DMPK properties of the series leading to **9b**, a potent, selective IGF-1R/IR dual inhibitor with favorable druglike properties. It possesses a profile comparable to that of OSI-906, including excellent PK and tolerability in multiple species and robust in vivo antitumor activity in several mouse xenograft tumor models.

SUPPORTING INFORMATION AVAILABLE Synthetic procedure, analytical data for compound **9b**, and procedures for in vitro and in vivo assays. This material is available free of charge via the Internet at http://pubs.acs.org.

DOI: 10.1021/ml100178g | *ACS Med. Chem. Lett.* **2010**, *1*, 510–515

AUTHOR INFORMATION

Corresponding Author: *To whom correspondence should be addressed. Tel: 631-962-0627. Fax: 631-845-5671. E-mail: mjin@OSIP.com (M.J.). Tel: 631-962-0787. Fax: 631-845-5671. E-mail: mmulvihill@OSIP.com (M.J.M.).

ACKNOWLEDGMENT We gratefully acknowledge Dr. Yingjie Li and Viorica M. Lazarescu for analytical support, Paul Maresca, Pete Meyn, Roy Turton, and the Leads Discovery Group for conducting in vitro ADMET studies, and Dr. Bob Zahler for consultation. We also gratefully acknowledge Dr. Andrew P. Crew for valuable discussions pertaining to the synthesis of the imidazo[5,1-*f*][1,2,4]triazine as well as Drs. Maryland Franklin and Qun-Sheng Ji for their overarching contributions to the OSI IGF-1R programs.

REFERENCES

(1) Adams, T. E.; Epa, V. C.; Garrett, T. P.; Ward, C. W. Structure and function of the type 1 insulin-like growth factor receptor. *Cell. Mol. Life Sci.* **2000,** *57*, 1050–1093.

(2) De Meyts, P.; Whittaker, J. Structural biology of insulin and IGF1 receptors: implications for drug design. *Nat. Rev. Drug Discovery* **2002,** *1*, 769–783.

(3) Buck, E.; Eyzaguirre, A.; Rosenfeld-Franklin, M.; et al. Feedback mechanisms promote cooperativity for small molecule inhibitors of epidermal and insulin-like growth factor receptors. *Cancer Res.* **2008,** *68*, 8322–8332.

(4) Garcia-Echeverria, C.; Pearson, M. A.; Marti, A.; et al. In vivo antitumor activity of NVP-AEW541-A novel, potent, and selective inhibitor of the IGF-IR kinase. *Cancer Cell* **2004,** 231–239.

(5) LeRoith, D.; Roberts, C. T., Jr. The insulin-like growth factor system and cancer. *Cancer Lett.* **2003,** *195*, 127–137.

(6) Martins, A. S.; Mackintosh, C.; Martin, D. H.; et al. Insulin-like growth factor I receptor pathway inhibition by ADW742, alone or in combination with imatinib, doxorubicin, or vincristine, is a novel therapeutic approach in Ewing tumor. *Clin. Cancer Res.* **2006,** 3532–3540.

(7) Pollak, M. Insulin and insulin-like growth factor signalling in neoplasia. *Nat. Rev. Cancer* **2008,** 915–928.

(8) Sell, C.; Rubini, M.; Rubin, R.; Liu, J. P.; Efstratiadis, A.; Baserga, R. Simian virus 40 large tumor antigen is unable to transform mouse embryonic fibroblasts lacking type 1 insulin-like growth factor receptor. *Proc. Natl. Acad. Sci. U.S.A.* **1993,** *90*, 11217–11221.

(9) Allen, G. W.; Saba, C.; Armstrong, E. A.; et al. Insulin-like growth factor-I receptor signaling blockade combined with radiation. *Cancer Res.* **2007,** *67*, 1155–1162.

(10) Cohen, B. D.; Baker., D. A.; Soderstrom., C.; et al. Combination therapy enhances the inhibition of tumor growth with the fully human anti-type 1 insulin-like growth factor receptor monoclonal antibody CP-751,871. *Clin. Cancer Res.* **2005,** *11*, 2063–2073.

(11) Guix, M.; Faber., A. C.; Wang, S. E.; et al. Acquired resistance to EGFR tyrosine kinase inhibitors in cancer cells is mediated by loss of IGF-binding proteins. *J. Clin. Invest.* **2008,** 2606–2619.

(12) Nahta, R.; Yuan, L. X.; Zhang, B.; Kobayashi, R.; Esteva, F. J. Insulin-like growth factor-I receptor/human epidermal growth factor receptor 2 heterodimerization contributes to trastuzumab resistance of breast cancer cells. *Cancer Res.* **2005,** *65*, 11118–11128.

(13) Zeng, X.; Sachdev, D.; Zhang, H.; Gaillard-Kelly, M.; Yee, D. Sequencing of type I insulin-like growth factor receptor inhibition affects chemotherapy response in vitro and in vivo. *Clin. Cancer Res.* **2009,** *15*, 2840–2849.

(14) Osborne, R. Commercial interest waxes for IGF-1 blockers. *Nat. Biotechnol.* **2008,** *26*, 719–720.

(15) Frasca, F.; Pandini, G.; Scalia, P.; et al. Insulin receptor isoform A, a newly recognized, high-affinity insulin-like growth factor II receptor in fetal and cancer cells. *Mol. Cell. Biol.* **1999,** *5*, 3278–3288.

(16) Giorgino, F.; Belfiore, A.; Milazzo, G.; et al. Overexpression of insulin receptors in fibroblast and ovary cells induces a ligand-mediated transformed phenotype. *Mol. Endocrinol.* **1991,** *3*, 452–459.

(17) Heuson, J. C.; Legros, N. Effect of insulin and of alloxan diabetes on growth of the rat mammary carcinoma in vivo. *Eur. J. Cancer* **1970,** *4*, 349–351.

(18) Kalli, K. R.; Falowo, O. I.; Bale, L. K.; Zschunke, M. A.; Roche, P. C.; Conover, C. A. Functional insulin receptors on human epithelial ovarian carcinoma cells: implications for IGF-II mitogenic signaling. *Endocrinology* **2002,** *143*, 3259–3267.

(19) Pavelic, K.; Pavelic, Z.; Poljak-Blazi, M.; Sverko, V. The effect of insulin on the growth of transplanted tumors in mice. *Biomedicine* **1979,** 125–127.

(20) Buck, E.; Gokhale, P.; Koujak, S.; Brown, E.; Eyzaguirre, A.; Tao, N.; Rosenfeld-Franklin, M.; Lerner, L.; Chiu, I.; Wild, R.; Pachter, J.; Epstein, D.; Miglarese, M. Compensatory insulin receptor (IR) activation upon inhibition of insulin-like growth factor receptor (IGF-1R): Rationale for co-targeting IGF-1R and IR in cancer. Abstract #1654, AACR Annual Meeting, Washington, DC, 2010.

(21) Li, R.; Pourpak, A.; Morris, S. W. Inhibition of the insulin-like growth factor-1 receptor (IGF1R) tyrosine kinase as a novel cancer therapy approach. *J. Med. Chem.* **2009,** *52*, 4981–5004.

(22) Mulvihill, M.; Ji, Q.; Coate, H.; Cooke, A.; Dong, H.; Feng, L.; Foreman, K.; Rosenfeld-Franklin, M.; Honda, A.; Mak, G.; Mulvihill, K.; Nigro, A.; O'Connor, M.; Pirrit, C.; Steinig, A.; Siu, K.; Stolz, K.; Sun, Y.; Tavares, P.; Yao, Y.; Gibson, N. Novel 2-phenylquinolin-7-yl-derived imidazo[1,5-*a*]pyrazines as potent insulin-like growth factor-I receptor (IGF-IR) inhibitors. *Bioorg. Med. Chem.* **2008,** *16*, 1359–1375.

(23) Mulvihill, M.; Cooke, A.; Rosenfeld-Franklin, M.; Buck, E.; Foreman, K.; Landfair, D.; O'Connor, M.; Pirrit, C.; Sun, Y.; Yao, Y.; Arnold, L.; Gibson, N.; Ji, Q. Discovery of OSI-906: A selective and orally efficacious dual inhibitor of the IGF-1 receptor and insulin receptor. *Future Med. Chem.* **2009,** *1*, 1153–1171.

(24) Werner, D. S.; Dong, H.; Kadalbajoo, M.; Laufer, R. S.; Tavares-Greco, P. A.; Volk, B. R.; Mulvihill, M. J.; Crew, A. P. Synthetic approaches to 5,7-disubstituted imidazo[5,1-*f*][1,2,4]triazin-4-amines. *Tetrahedron Lett.* **2010,** 3899–2901.

(25) Altering the inhibitor structure from PQIP (PDB ID 3D94) by deleting the attachment off the cyclobutyl moiety and modifying the 5-position of the imidazopyrazine from CH to N yields the depicted model.

(26) Ji, Q.; Mulvihill, M.; Rosenfeld-Franklin, M.; Cooke, A.; Feng, L.; Mak, G.; O'Connor, M.; Yao, Y.; Pirritt, C.; Buck, E.; Eyzaguirre, A.; Arnold, L.; Gibson, N.; Pachter, J. A novel, potent, and selective insulin-like growth factor-I receptor kinase inhibitor blocks insulin-like growth factor-I receptor signaling in vitro and inhibits insulin-like growth factor-I receptor dependent tumor growth in vivo. *Mol. Cancer Ther.* **2007,** *6*, 2158–2167.

(27) Lerner, L.; Liu, Q.; Yang, J.; et al. et al. Generation of in vivo tumor models driven by Insulin-Like Growth Factor Receptor IGF1R and their use in the development of OSI-906, a selective IGF1R inhibitor. Abstracts A233, AACR-NCI-EORTC International Conference: Molecular Targets and Cancer Therapeutics, Nov 15−19, 2009, Boston, MA.

(28) See the Supporting Information.

DOI: 10.1021/ml100178g | *ACS Med. Chem. Lett.* **2010,** *1*, 510–515